Improved therapeutic window in *BRCA* mutant tumors with antibody linked pyrrolobenzodiazepine dimers with and without PARP inhibition

Haihong Zhong[1]*, Cui Chen[1], Ravinder Tammali[1], Shannon Breen[1], Jing Zhang[1], Christine Fazenbaker[1], Maureen Kennedy[1], James Conway[1], Brandon W. Higgs[1], Nicholas Holoweckyj[1], Rajiv Raja[1], Jay Harper[1], Andrew J. Pierce[2], Ronald Herbst[1], and David A. Tice[1]*

Affiliations: [1]Oncology Research; [2]Translational Science; MedImmune, Gaithersburg, Maryland 20850

[2]Translational Science – Oncology, Innovative Medicines and Early Development, AstraZeneca, Cambridge, UK

Running title: Targeting BRCA mutated tumors with PBD-based ADC plus PARPi

Keywords: BRCA, DNA damage repair, antibody drug conjugate, pyrrolobenzodiazepine dimers (PBD), olaparib, combination therapy,

Financial support: All authors are full time employees of MedImmune (AztraZeneca). This work was supported by Medimmune

*** Corresponding Authors:**

Haihong Zhong
Oncology Research
Medimmune
One Medimmune Way
Gaithersburg, MD 20878
Phone: 301-398-5343
Email: zhongh@medimmune.com

David A. Tice
Oncology Research
Medimmune
One Medimmune Way
Gaithersburg, MD 20878
Phone: 301-398-4592
ticed@medimmune.com

Conflict of interest: no conflicts of interest to disclose

Word count (excluding references):

No. of Tables / figures: 5 Figures

Abstract

Pyrrolobenzodiazepine dimers (PBDs) form cross-links within the minor groove of DNA causing double strand breaks (DSB). DNA repair genes such as *BRCA1* and *BRCA2* play important roles in homologous recombination repair of DSB. We hypothesized that PBD-based antibody drug conjugates (ADCs) will have enhanced killing of cells in which homologous recombination processes are defective by inactivation of *BRCA1* or *BRCA2* genes. To support this hypothesis, we found 5T4-PBD, a PBD-dimer conjugated to anti-5T4 antibody, elicited more potent antitumor activity in tumor xenografts that carry defects in DNA repair due to *BRCA* mutations compared to *BRCA* wild-type xenografts. To delineate the role of *BRCA1/2* mutations in determining sensitivity to PBD, we used siRNA knockdown and isogenic *BRCA1/2*-knockout models to demonstrate that *BRCA* deficiency markedly increased cell sensitivity to PBD-based ADCs. To understand the translational potential of treating patients with *BRCA* deficiency using PBD-based ADCs, we conducted a “mouse clinical trial” on 23 patient-derived xenograft (PDX) models bearing mutations in *BRCA1* or *BRCA2*. 61-74% PDX models had tumor stasis or regression when treated with a single dose of 0.3 mg/kg or three fractionated doses of 0.1 mg/kg of a PBD-based ADC. Furthermore, suboptimal dose of PBD-based ADC in combination with olaparib resulted in significantly improved antitumor effects was not associated with myelotoxicity and was well tolerated. In conclusion, PBD-based ADC alone or in combination with a PARP inhibitor may have improved therapeutic window in cancer patients carrying *BRCA* mutations.

Introduction

Antibody-drug conjugates (ADCs) are an emerging novel class of anticancer treatment agents that provide improved target specificity and potency. Four ADCs have been approved so far, ado-trastuzumab emtansine, brentuximab vedotin, inotuzumab ozogamicin, and gemtuzumab ozogamicin. However, most ADCs still fail due to dose-limiting toxicities on critical normal tissues occurring at doses too low to achieve antitumor activity (1). Therefore, one of the major challenges to ADCs is the narrow therapeutic index. In recent years, significant advances in engineering new linker and conjugation technologies together with novel highly cytotoxic payload have been made in an effort to develop safer, more effective ADCs**.** Most cytotoxic payloads used in ADCs currently under investigation are microtubule inhibitors and DNA-damaging drugs. The tubulin inhibitors, such as auristatin and maytansinoid, are potent cytotoxic agents against cultured cancer cells, with IC_{50} values in the picomolar range as free drugs (2, 3). The DNA-damaging agents, such as duocarmycin and calicheamicin are powerful antitumor antibiotics that bind to the minor groove of DNA. Another new category of DNA-damaging agent is pyrrolobenzodiazepine dimers (PBDs). PBD dimers bind in the minor groove of DNA and crosslink opposite strands causing double stand breaks (DSB) (4). It has been shown that PBD dimers have very potent cytotoxicity with 10-fold lower IC_{50} compared to auristatins and maytansinoids with activity against a broad spectrum of tumors (5, 6, 7, 8). PBD dimers and PBD-based ADCs are currently being evaluated in clinical trials with more anticipated to enter clinical development over the next few years (9, 10, 11).

The repair of DSB is accomplished by two main DNA damage repair mechanisms: homologous recombination (HR) and non-homologous end joining (NHEJ). HR uses a homologous DNA template and can repair DSB with high fidelity. BRCA1 and BRCA2 are key mediators involved in repairing DSB via HR (12). When mutated, these genes are associated with familial breast and ovarian cancer. Approximately 10% to 20% of breast and ovarian cancers are attributed to germline mutations in *BRCA1/2* genes (13, 14). Normal tissues are heterozygous and retain a wild-type copy of the *BRCA* gene, while tumors lose the functional allele and become homozygous for *BRCA* deficiency. *BRCA* mutated cells exhibit enhanced sensitivity to DNA interstrand crosslinking agents including platinum-based chemotherapeutic drugs, melphalan, topoisomerase II inhibitors, and inhibitors of poly-ADP-ribosylation (PARP) (15, 16). PARP is a DNA binding protein that binds and removes the damaged region of DNA (17). PARP inhibitors (PARPi) have been shown to induce synthetic lethality in *BRCA*-mutated cancer cells (18, 19). In the clinic, PARPi, such as olaparib and rucaparib, significantly improved progression-free survival in patients with germline *BRCA* mutations as single agent, and have gained FDA approval (20, 21, 22). Other PARPi, including veliparib, talazoparib, and niraparib, are currently being accessed in clinical trials and showed promising results (23, 24, 25). Despite the profound and sustained anti-tumor response in patients harboring *BRCA* mutations, PARPi has not yet demonstrated significant improvement in overall survival (26, 27, 28). PARPi combination therapy has been evaluated extensively over the last decade. A number of preclinical studies have shown that PARP inhibition can enhance the effects of agents that induce DNA damage such as ionizing radiation and some chemotherapeutics in cancer types such as breast, ovarian, lung, melanoma, and prostate cancers (29, 30, 31, 32, 33). This includes the first combination of a PARPi with an ADC, IMMU-132, which employs a topoisomerase I inhibitor (34).

We hypothesized that since PBD dimers cause DNA damage by crosslinking, that PBD-based ADCs will have enhanced killing of cells in which HR processes are defective by inactivation of *BRCA1* or *BRCA2* genes. In this paper, we provide evidence that knocking down or mutating *BRCA1* or *BRCA2* genes by genetic approaches sensitized cells to PBD and a PBD-based ADC. In addition, enhanced efficacy was observed upon combining olaparib with a less than full monotherapy dose of PBD-based ADC in *BRCA2*-deleted xenograft models. Furthermore, combination therapy was not associated with myelotoxicity and was well tolerated in mice, indicating an improved therapeutic window. The marked sensitivity of *BRCA*-deficient tumors to PBD-based ADC alone and its combination with PARP inhibitor may have important implications for optimal treatment of breast and ovarian cancer patients carrying *BRCA* mutations.

Materials and Methods

Cells and Reagents

Breast cancer cell lines MDA-MB-361, SUM149PT, MDA-MB-436, pancreatic cancer cell line Capan-1, and Hela cells were purchased from American Type Culture Collection (Manassas, VA). DLD-1, DLD-1 *BRCA2-/-*, MCF10A, and MCF10A *BRCA1*(185delAG/+) cells were purchased from Horizon Discovery Ltd (Cambridge, United Kingdom). Upon delivery, cells were expanded and low passage vials were stored in liquid nitrogen. Studies were carried out within 8 weeks after resuscitation. Cell line authentication was conducted using STR-based DNA fingerprinting and multiplex PCR. IMPACT tests were also performed on all cell lines. CellTiter-Glo (CTG) reagents were obtained from Promega (Madison, WI). For *in vitro* studies, Olaparib (LC Laboratories, Woburn, MA, USA) was dissolved in DMSO and diluted by culture media before use. ELISA kits for γH2AX were purchased from R&D Systems (Minneapolis, MN).

γH2AX Immunofluorescence and ELISA assay

γH2AX immunofluorescence staining was done using a chamber slide staining assay. DLD-1 and DLD-1 *BRCA2*-/- were plated 25,000 cells/well in 8-well, collagen coated chamber slides in 10%FBS DMEM medium. On the next day, medium containing 1 μg/ml cisplatin or 10 ng/ml 5T4-PBD or 100 ng/ml 5T4-PBD were added to the treatment wells. After 24 hr, cells were fixed and permeabilized. Cells were then incubated with primary antibody (phospo-histone H2A.X, Cell Signaling Technology) at room temperature for 1 hr, followed by incubation with secondary antibody (goat anti-rabbit IgG (H+L) Alexa Fluor 647 conjugate, Thermo Fisher Scientific) for 1 hr, and mounted using DAPI-containing mounting media. Images were captured using a confocal microscope.

γH2AX pharmacodynamic assay kit was purchased from Trevigen, Inc. Assay was performed following the protocol established by the manufacturer.

siRNA Knockdown Experiment

HeLa cells were transfected with siRNA directed against *BRCA1* or *BRCA2* genes (ON-TARGETplus SMARTpool reagents, Dharmacon) and a negative control *GAPDH* gene (ON-TARGETplus siCONTROL Non-targeting Pool reagent, Dharmacon) using RNAiMax transfection reagent (Life Technologies) for 48 hr according to manufacturer’s instructions. After that, cells were treated with either PBD (SG3199) or 5T4-PBD in the medium containing 10% FBS for 5 days. Cell viability was measured by Cell Titer Glow reagent (Promega).

qRT-PCR Analysis

HeLa cells were transfected using siRNA directed against *BRCA1*, *BRCA2*, and *GAPDH* genes as described above. After 48 hr, cells were lysed using Cells to Ct kit (Ambion) and qRT-PCR analysis was performed with EXPRESS One-Step Superscript qRT-PCR Kit using probes against *BRCA1*, *BRCA2*, and *GAPDH*. 18S rRNA was used as a housekeeping gene for normalization of samples (Thermo Fisher Scientific).

BRCA Mutation Characterization in PDX Tumors

Whole exome sequencing (WES) was performed on 23 patient-derived xenograft samples. DNA was isolated using QIAamp DNA Mini Kit (Qiagen, Germantown, MD) and 3 µgs were randomly fragmented to an average peak size of 200bp using Covaris M220 (Covaris, Woburn, MA). Agilent Sure Select Human All Exon V6 baits were utilized for exome capture and the WES library preparation was performed following the manufacture's protocol (*Agilent SureSelect^{XT} Target Enrichment System for Illumina Multiplexed Sequencing*). The quality and quantity of the libraries were evaluated using an Agilent Bioanalyzer 2200 (Agilent, Santa Clara, CA) in conjunction with KAPA Library Quantification Kit (Kapa Biosystems, Wilmington, MA). The WES libraries were sequenced on an Illumina NextSeq 500 instrument at 2 x 100bp using NextSeq 500/550 v2 reagent kits (Illumina, San Diego, CA).

Sequencing reads were aligned to the human hg19 reference genome (UCSC hg19; Feb 2009 release; Genome Reference Consortium GRCh37) using Bowtie 2 (35). Duplicate reads were identified and removed using Picard. Samtools was applied to bam files from all PDX models to create a single summary of coverage for mapped reads. Bcftools was used to call variants and generate a single VCF file for all PDX models. Functional annotation was assigned to variants with ANNOVAR, which assigned annotation from selected databases (RefGene, 1000 Genome Project, Phast Cons, Genomic Super Dups, ESP6500, LBJ and COSMIC). Variants were filtered to include only nosynonymous, stop gain or loss, or frameshift insertion or deletion. Variants were further filtered to include only rare occurrences by retaining variants with MAF≤0.05, or no presence in the 1000 Genome Project database.

Raw sequencing data has been deposited in SRA database. The accession number is PRJNA494524.

Xenograft Studies in Mice

All procedures using mice were approved by the MedImmune Institutional Animal Care and Use Committee according to established guidelines. For *in vivo* efficacy studies, 5 or 10 million cells in 50% matrigel were inoculated subcutaneously into female athymic nude mice (Harlon Laboratories). When tumors reached approximately 150-200 mm^3, mice were randomly assigned into groups (8-10 mice per group). 5T4-PBD was administered intravenously as a single dose at indicated doses. Olaparib was solubilized in DMSO and diluted in water containing 15% Hydroxypropyl betadex (Sigma, St. Louis, MO) before administering by oral gavage daily at indicated dose. Tumor volumes were measured twice weekly with calipers. Tumor growth inhibition was calculated using the formula ½ x L x W^2 (L = length; W = width). Body weights were measured twice weekly to assess tolerability of the treatments. Two-way ANOVA was used to compare the reduction in tumor volume in mice treated with the combination therapies versus those treated with either agent alone.

For hematologic toxicity study, athymic *nu/nu* nude mice received either olaparib (100 mg/kg, oral gavage, day 0-15), or 5T4-PBD (0.1 mg/kg, iv, single dose on day 0), or the combination of both. Whole blood (50 μl) was drawn through orbital bleeding and was transferred to EDTA tubes. Complete blood count was determined using the Sysmex XT-2000 hematology analyzer.

Results

Enhanced killing of *BRCA-1* or *BRCA-2* deficient xenograft tumors compared to *BRCA* wild-type tumors

5T4-PBD (MEDI0641) is an ADC in which anti-5T4 antibody was site-specifically conjugated to two PBD dimers (SG3249) per antibody. It has been shown to elicit a potent anti-tumor response in 5T4-positive xenograft models (36). In the process of characterizing 5T4-PBD, we noticed that it had superior anti-tumor activity in the models that carry *BRCA* mutations. To fully understand the efficacy of the PBD-based ADC in *BRCA* mutated xenograft tumors, we established *BRCA* wild-type and *BRCA* mutated xenograft models. *BRCA* wild-type xenografts include two breast cancer models that have high 5T4 surface expression (MDA-MB-361, MDA-MB-468) and one lung cancer model NCI-H1975 with low to medium 5T4 expression. *BRCA* mutated xenograft models include two breast cancer models with *BRCA1* mutation that express high or medium levels of surface 5T4 (SUM149PT and MDA-MB-436), and one pancreatic cancer xenograft model that has low levels of surface 5T4 and is *BRCA2* deficient (Capan-1). Treatment of mice bearing *BRCA* wild-type xenografts with a single dose of 5T4-PBD at 0.3 mg/kg resulted in tumor stasis followed by tumor regrowth (Figure 1A). However, treatment of mice bearing BRCA mutated xenografts with a single dose of 5T4-PBD at 0.3 mg/kg resulted in tumor regression (Figure 1B). Even treatment with the low dose of 0.1 mg/kg resulted in tumor regression in two of the BRCA deficient models. Isotype control ADC demonstrated more impact in *BRCA* mutant models compared to wild type again suggesting that the cells are more sensitive to the PBD regardless of whether it enters the cell in a target-specific or non-specific manner. Overall, the PBD-based ADC was more potent in *BRCA* deficient xenograft models compared to wild type xenografts, regardless of target expression levels consistent with a role for BRCA1/2 in repair of DNA interstrand crosslinks and related downstream DNA damage

DNA repair defects from genetic deletion of *BRCA1/2* markedly increases anti-tumor activity of a PBD-based ADC

To investigate BRCA as a determinant of sensitivity to PBD, we used siRNA to knockdown *BRCA1* or *BRCA2* genes in DNA repair wild type Hela cells. Quantitative PCR and western blot demonstrated nearly complete depletion of BRCA1 and BRCA2 at mRNA and protein levels. Suppression of BRCA1 or BRCA2 resulted in 5- to 10-fold increase in sensitivity to PBD and 5T4-PBD (Supplemental Figure S1).

To further demonstrate the role of *BRCA* genes in determining sensitivity to PBD-based ADCs, we used isogenic models of *BRCA1* or *BRCA2* deficiency. MCF10A *BRCA1*(185delAG/+) is a breast epithelial cell line with heterozygous knockin of a 2-bp deletion resulting in a premature stop codon at position 39 terminating BRCA1 protein expression (37) *vs.* the *BRCA1* wild-type parental MCF10A line. DLD1 *BRCA2*-/- is a colorectal adenocarcinoma cell line with homozygous deletion of exon 11 of the *BRCA2* gene (15), engineered from *BRCA2* wild-type DLD1 cells. The use of isogenic cell pairs allowed us to exclude many other unknown factors that could contribute to the differential sensitivity in nonisogenic systems. FACS analysis demonstrated that both parental and *BRCA*-deficient cells had equivalent 5T4 surface expression (Figure 2A, Supplemental Figure S2A). MCF10A *BRCA1*(185delAG/+) and DLD1 *BRCA2*-/- cells were 5-fold and 24-fold more sensitive to 5T4-PBD in cytotoxicity assays compared with their wild-type cells, respectively (Figure 2B, Supplemental Figure S2B).

To examine effects of *BRCA* deficiency on antitumor activity *in vivo*, we grew DLD1 parental and DLD1 *BRCA2*-/- xenografts subcutaneously in nude mice and compared tumor growth following administration of a single dose of 5T4-PBD at 0.1, 0.3, and 1 mg/kg. 0.1 mg/kg of 5T4-PBD was inactive against DLD1 wild-type tumor. There was modest tumor growth inhibition of DLD1 tumors observed with 5T4-PBD treatment at 0.3 and 1.0 mg/kg (Figure 2C, top panel). In contrast, even though DLD1 *BRCA2*-/- tumors grew slower than DLD1 wild-type parental tumors, a single dose of 5T4-PBD at 0.1 mg/kg significantly inhibited growth of DLD1 *BRCA2*-/- tumor xenografts, with tumor regression seen at 0.3 and 1.0 mg/kg (Figure 2C, bottom panel), suggesting *BRCA2* deficiency markedly sensitized DLD1 tumors to the DNA damage caused by the PBD-based ADC.

To examine the extent of DNA damage in response to PBD-based ADC treatment, we evaluated γH2AX foci formation, a well-established biomarker of DNA damage (38). γH2AX immunofluorescence staining was notably stronger in *BRCA2*-/- cells as compared with wild-type cells upon 5T4-PBD treatment (Figure 2D). We also quantified expression of γH2AX protein using an ELISA-based γH2AX pharmacodynamic assay. Expression of γH2AX was elevated in all treatment groups compared with untreated control in both DLD1 *BRCA2*-/- and wild-type lines, however, the increase associated with 5T4-PBD treatment in *BRCA2*-/- cells was statistically significant (Figure 2D). Interestingly, increased γH2AX were readily detected in untreated *BRCA2*-/- cells compared to untreated parental cells consistent with an intrinsic HR defect.

Of interest, we noticed that baseline levels of other HR repair (HRR) proteins such as FANCD2, Rad51, BARD1, and DNA excision repair protein ERCC1 were higher in DLD1 cells than those in DLD1 *BRCA2*-/- cells (Figure 2E). It is possible that the high expression of other HRR proteins in DLD1 cells may result in more efficient repair of damaged DNA induced by 5T4-PBD. The decreased expression of HRR proteins in DLD1 *BRCA2*-/- cells may contribute to the greater sensitivity to PBD-based ADC. DLD1 *BRCA2*-/- cells also had increased protein expression of PARP1 compared to parental DLD1 cells.

Pharmacologic response across *BRCA* deficient PDX models

To understand the translational potential of treating patients with *BRCA* deficiency using PBD-based ADCs, we collected 23 breast and ovarian patient-derived xenograft models that were deficient for either *BRCA1* (n=12) or *BRCA2* (n=6) or both genes (n=5) (Supplemental Table S1) and assessed the efficacy of 5T4-PBD. Mice were treated with 5T4-PBD administered as either a single dose of 0.3 mg/kg or as three fractionated doses of 0.1 mg/kg. When administered as single dose at 0.3 mg/kg, 17 PDXs (73.9% DCR (disease control rate)) demonstrated complete regression (CR), partial regression (PR), and stable disease (SD) (Supplemental Figure S3). We then tested the dosing regimen of 0.1 mg/kg given every 3 weeks for a total of 3 doses. DCR rate was 60.8% (14 out of 23 models). In some models, tumor regressions including CRs were already observed after first dose of 0.1 mg/kg (Supplemental Figure S3). In contrast, neither dosing regimen resulted in a response in 3 *BRCA* wild-type PDX models (Supplemental Figure S4). The 5T4-PBD was well tolerated with no body weight loss reported in any of the PDX models.

We performed retrospective analysis of 5T4 expression in untreated PDX tumors using methods previously described (36). IHC analysis demonstrated a wide range of 5T4 staining patterns across 23 *BRCA*-deficient and 3 *BRCA*-wild type PDX models. Each tumor was assessed with membrane staining and given two scores, intensity score (IS, 1+, 2+, 3+) and frequency score (FS, proportion of positive tumor cells across majority of section where 1 is < 10% of tumor cells staining positive, 2 = 11-24%, 3 = 25-49%, 4 = 50-75% and 5 = >75%)). The final IHC score of each tumor was calculated using the formula of IS x FS. The tumors were then divided into 3 groups based on the following criteria: (i) IHC score 1 had IS x FS score $\leq$ 5; (ii) IHC score 2 was categorized as $5 <$ IS x FS ≤ 10; (iii) $10 <$ IS x FS ≤ 15 was considered as IHC score 3. Representative IHC images are shown in Supplemental Figure S5. Figure 3 depicts waterfall plots of the anti-tumor effect of 5T4-PBD dosed at 0.3 and 0.1 mg/kg with an integration of the IHC scores for each PDX model. The data indicated no correlation between 5T4 expression and sensitivity to 5T4-PBD in these *BRCA*-deficient PDX tumors.

Combination with olaparib further enhances the anti-tumor activity of a PBD-based ADC in *BRCA2-/-* tumors

BRCA-deficient cells are known to be more sensitive to PARP inhibitors compared with wild-type *BRCA* cells (18, 19). Using DLD1 isogenic cells, we found similar to published results that *BRCA2-/-* cells were as much as over 200-fold more sensitive to olaparib compared to *BRCA* wild-type cells in a cytotoxicity assay (Figure 4A).

The findings demonstrating an increased sensitivity of *BRCA* mutated cells to either PBD-based ADCs or olaparib prompted us to consider combination strategies that could potentially lead to an enhanced anti-tumor effect compared to single agent therapy. We first used *in vitro* cytotoxicity assays to evaluate the efficacy of sub-optimal doses of 5T4-PBD and olaparib alone or in combination in DLD1 parental and *BRCA2-/-* cells. In DLD1 parental cells, a minimal cytotoxic effect was observed with combination treatment. However, in *BRCA2-/-* cells, when 5T4-PBD was combined with olaparib, a significantly higher percentage of cell death was induced compared with either agent alone (Figure 4B).

The combination of 5T4-PBD with olaparib was also assessed *in vivo* in the DLD1 and DLD1 *BRCA2*-/- xenograft models. In the DLD1 xenograft model, olaparib had a minimal effect on tumor growth whereas 5T4-PBD dosed at a high dose of 1 mg/kg showed 66% tumor growth inhibition. However, the combination failed to improve efficacy in this model (Figure 4C, left panel). On the other hand, olaparib demonstrated some degree of anti-tumor activity in the DLD1 *BRCA2*-/- xenograft model (59% TGI) (Figure 4D, left panel). Consistent with the data in Figure 2C, 5T4-PBD treatment was efficacious as a single agent at a dose as low as 0.1 mg/kg in DLD1 *BRCA2*-/- tumor (69% TGI). Combining olaparib with 0.1 mg/kg 5T4-PBD resulted in tumor regression (111% TGI), a significantly improved efficacy compared to either single agent alone (Figure 4D, left panel). We also noticed that animals in the 5T4-PBD or combination treatment groups showed body weight gain compared to those treated with olaparib alone. This trend was much more obvious in mice bearing DLD1 *BRCA2*-/- tumor, suggesting a benefit of the combination in tolerability/safety in addition to efficacy (Figure 4D, right panel), perhaps in part due to significantly reduced tumor burden.

Combination of PBD-based ADC and olaparib is not associated with any increased hematological toxicity compared to single agent alone

Olaparib toxicities in human include thrombocytopenia and grade 3 fatigue (39). In preclinical toxicity studies, the primary target organ of olaparib was bone marrow, with associated changes in peripheral hematology parameters. Currently, only a limited number of PBD-based ADCs are in clinical trials. Initial toxicities that have been reported include neutropenia, low platelet counts, and skin rash (10, 11). We decided to look at the hematologic profile of combining olaparib with 5T4-PBD to see whether the combination would be associated with any increased toxicities. We did the study in naïve mice to examine the possible off-target toxicities as 5T4 antibody does not cross react with the mouse 5T4 antigen. The doses and dosing schedule were the same as used in the DLD1 *BRCA2-/-* efficacy study at which optimal antitumor activity was observed (Figure 4D). On day 0, mice were administered a single dose of 5T4-PBD at 0.1 mg/kg and daily olaparib therapy (100 mg/kg) up to day 15. Blood samples were collected at indicated time points and complete blood counts were measured. Despite some significant decreases in WBC, monocyte, and lymphocyte upon olaparib treatment on day 9, the counts all recovered once olaparib dosing was stopped (day 20, day 27) (Figure 5). Mice treated with 5T4-PBD monotherapy did not demonstrate changes in any parameters up to day 27 (Figure 5). Importantly, olaparib plus 5T4-PBD treatment was well tolerated. The only significant drop was found in monocyte counts on day 9, which mirrored the olaparib single agent showing full recovery after olaparib dosing was stopped (day 20, day 27) (Figure 5). Together, the results indicate that the combination of olaparib with low dose level of 5T4-PBD improves efficacy as demonstrated in Figure 4D, and does not cause significant myelotoxicity. It further suggests a wider therapeutic window for the combination strategy in treating *BRCA* mutated tumors.

Discussion

The concept of an ADC is to direct the action of the chemotherapeutic drug to maximize the impact in tumor while minimizing the damage to normal tissues. While some clinical success and validation of this technology has been realized, the vast majority of ADCs have failed in the clinic due to lack of therapeutic index. These failures appear to be independent of the target or technology employed. All classes of warheads have suffered clinical failures, including several recent failures by PBD-based ADCs, largely due to toxicity typically associated with the cytotoxic agent. Advances in ADC technology continue to offer promise to widen the therapeutic index. Similarly, a better understanding of the underlying biology and mechanisms of action of the cytotoxic agents may provide opportunity to widen the therapeutic index of ADCs. Herein we provide further evidence that tumor cells with underlying defects in DNA damage response (DDR) pathways, such as mutation or loss of *BRCA1/2*, may be hypersensitive to PBD based ADCs. Likewise, combinations with inhibitors of DDR pathways such as the PARPi olaparib demonstrated here, can further enhance the antitumor activity. This supports testing expanded patient selection strategies for ADCs beyond just target expression and to think about rational combination strategies based on warhead mechanism of action as a way to further enhance the therapeutic index of ADCs.

In this study 5T4-PBD was used as an exemplary ADC to further explore these hypotheses in preclinical models. 5T4 is a target of both active and failed ADCs and has been well characterized as an ADC target in preclinical models (36). Therefore, it served as a logical surrogate in these studies to deliver the PBD payload to tumor cells. The mechanism of action of the PBD is expected to be the critical factor when exploring biomarkers of activity and drug combination strategies. To this end, we did not observe any dependence on 5T4 expression levels provided that it was expressed at a sufficient level to deliver PBD inside the cell. This finding is consistent with the results previously reported by Sutherland et al who demonstrated that CD33A-PBD retained potent cytotoxicity even in cells with low expression of CD33 (40). Cell models that do not express 5T4 do not show the same effects (Supplemental Figure S6) and activity was observed well above control IgG-PBD so it is anticipated that target expression is still a critical variable to consider in patient selection.

The strengths of this study include the use of a panel of *BRCA*-deficient PDX models that allowed us to test the clinical potential of this treatment protocol. Cell line xenograft models are generally not considered reliable predictors of clinical activity due to the clonal selection process on plastic. Patient-derived xenografts, on the other hand, recapitulate the genetic diversity found in human tumors and properly mimic intratumoral heterogeneity. Confidence in preclinical outcomes can be greatly increased by using a panel of PDX models for each tumor type. In our case, we selected 23 breast or ovarian PDX models based on their *BRCA* gene deficient status, and were blinded to target 5T4 expression. We demonstrated that a single dose of PBD-based ADC at 0.3 mg/kg induced tumor regression with DCR of 74% in *BRCA* deficient PDX models. Three fractionated doses of 0.1 mg/kg administered every 3 weeks resulted in similar DCR of 61%. Lower dose of ADC and increased dosing intervals may further minimize ADC-induced toxicity, as we have previously shown that fractionated dosing improved tolerability of PBD-based ADCs without impacting anti-tumor activity (41). Although our study is focused on breast and ovarian cancer, we expect that our results can be extended to other *BRCA* mutated cancers, such as prostate and pancreatic tumors, that are vulnerable to PBD-based ADCs.

Even though the PBD-based ADC demonstrated impressive anti-tumor efficacy in the majority of *BRCA*-mutant tumors in our study, some *BRCA* mutated tumors did not respond regardless of target expression level. It is possible that some tumors may require defects in more DNA repair proteins in addition to *BRCA* in order to demonstrate hypersensitivity to PBD treatment. In fact, our finding showing decreased expression of multiple DDR proteins in DLD1 *BRCA2*-/- cells suggests that defects in other DDR proteins may contribute to the high sensitivity observed with PBD-based ADC in *BRCA* deficient cells (Figure 2E). Previously, McCabe et.al showed that the sensitivity of *BRCA*-deficient cells to PARP inhibition was due to a defect in DNA damage signaling proteins, such as RAD51, RAD54, DSS1, RPA1, NBS1, ATR, ATM, CHK1, CHK2, FANCD2, FANCA, or FANCC, rather than a deficiency in BRCA1 or BRCA2 per se (42). Similarly, loss of tumor suppressor INPP4B resulted in a DNA repair defect and increased sensitivity to PARP inhibitor due to concomitant loss of BRCA1, ATR, and ATM (43). Interestingly, many of the PDX models examined in our study also carry mutations including PTEN, p53, ATM, and ATR. Further characterization of other DDR proteins or oncogenic pathways and understanding how they are associated with response to PBD-based

ADC is currently underway. It is our hope to identify other genes besides *BRCA1/2* that may contribute to the “BRCAness” of tumors, and to understand how other signaling pathways interplay with DDR pathway and whether this can be therapeutically exploited.

Following PBD-based ADC treatment, the *BRCA*-mutated cancer cells are unable to repair DSB and undergo cell death, or the cells rely on the base excision machinery to repair PBD-based damage via the enzyme PARP. PARP inhibitors have been shown to effectively kill *BRCA* deficient tumors by preventing cells from repairing DNA. Therefore, we hypothesized that the anti-tumor effect of PBD-based ADC in *BRCA*-mutated tumors could be further enhanced with concomitant PARP inhibition. By combining PBD-based ADC with a PARPi, there would be an increased accumulation of DSB due to the inability of DNA repair pathways to repair the damage with high fidelity, therefore causing cell death. Approaches combining PARPi with other DNA-damaging agents have been explored. A number of preclinical studies in various cancer types, such as breast, ovarian, and prostate cancer, have shown that PARP inhibition can enhance the effects of some chemotherapies and ionizing radiation. In addition to agents that directly interact with DNA and cause DSB, agents that inhibit topoisomerse 1, such as irinotecan, have been shown to synergize with PARPi. Recently, Cardillo et.al demonstrated that combining the anti-Trop-2-SN-38 ADC (IMMU-132) with PARPi resulted in synergistic growth inhibition in triple negative breast cancer tumors, regardless of *BRCA1/2* status (34). Here, we show that suboptimal dose of PBD-based ADC in combination with olaparib resulted in significantly enhanced antitumor effects compared to monotherapy in mice bearing *BRCA2*-deleted tumors. While *BRCA* wild-type tumors can still respond to PBD-based ADCs at significantly higher doses, these tumors do not respond to PARPi monotherapy. Consequently, we did not observe any synergy in this setting with the combination treatment, unlike in *BRCA*-mutated tumors. This contrasts with the observation by Cardillo et al suggesting there may either be differences in how cells repair damage induced by SN-38 compared to PBD or that other differences exist between DDR pathways used in the cell line models.

Since the therapeutic window is determined by efficacy and safety, the tolerability of PBD-based ADC in combination with olaparib was also evaluated in tumor-bearing and naïve mice. One noteworthy finding from our tolerability study was that 5T4-PBD plus olaparib combination therapy was well-tolerated in mice, with no effect on body weight change and little evidence of hematologic toxicity during and after the course of treatment. Together, the data demonstrate the potential for an increased therapeutic window by combining PBD-based ADC with a PARPi, as a result of significantly enhanced efficacy and improved tolerability in treating a subset of patients with *BRCA* deficient cancers. The combination strategy may be particularly advantageous for indications in which PARPi has been approved.

In conclusion, here we demonstrate that both *BRCA1* and *BRCA2* mutation status are key factors in determining the sensitivity to PBD-based ADCs. Our results show a markedly increased sensitivity to PBD-based ADC in *BRCA* deficient tumors. Moreover, we have demonstrated that PBD-based ADC in combination with PARPi has a widened therapeutic window with improved efficacy and better tolerability in treating *BRCA* deficient tumors. These results suggest a novel strategy for treating patients with *BRCA*-mutated tumors.

Acknowledgements

The authors thank colleagues from Spirogen and Medimmune ADPE department for synthesizing PBD payload and completing ADC conjugations, Steven Durant from the olaparib team and Gareth Davies for helpful discussion. We also thank Xentech, Champions, and South Texas Accelerated Research Therapeutics (START) for conducting in vivo experiments in patient-derived xenograft (PDX) models under service agreements.

References

1. Tolcher AW. Antibody drug conjugates: lessons from 20 years of clinical experience. Ann Oncol. 2016; 27(12): 2168-2172.

2. Gerber HP, Kung-Sutherland M, Stone I, Morris-Tilden C, Miyamoto J, McCormick R, Alley SC, Okeley N, Hayes B, Hernandez-Ilizaliturri FJ, McDonagh CF, Carter PJ, Benjamin D, Grewal IS. Potent antitumor activity of the anti-CD19 auristatin antibody drug conjugate hBU12-vcMMAE against rituximab-sensitive and -resistant lymphomas. Blood 2009;113(18): 4352–4361.

3. Lambert JM, Chari RV. Ado-trastuzumab Emtansine (T-DM1): An Antibody−Drug Conjugate (ADC) for HER2-Positive Breast Cancer). J Med Chem 2014;57: 6949-64.

4. Bose DS, Thompson AS, Ching J, Hartley JA, Berardini MD, Jenkins TC, Neidle S, Hurley LH, Thurston DE. Rational design of a highly efficient irreversible DNA interstrand cross-linking agent based on the pyrrolobenzodiazepine ring system. J Am Chem Soc 1992;114:4939-41.

5. Gregson SJ, Howard PW, Hartley JA, Brooks NA, Adams LJ, Jenkins TC, Kelland LR, Thurston DE. Design, synthesis, and evaluation of a novel pyrrolobenzodiazepine DNA-interactive agent with highly efficient cross-linking ability and potent cytotoxicity. J Med Chem 2001; 44(5):737-48.

6. Hartley JA, Spanswick VJ, Brooks N, Clingen PH, McHugh PJ, et al. SJG-136 (NSC 694501), a novel rationally designed DNA minor groove interstrand cross-linking agent with potent and broad spectrum antitumor activity: part 1: cellular pharmacology, in vitro and initial in vivo antitumor activity. Cancer Res 2004;64:6693-9.

7. Alley MC, Hollingshead MG, Pacula-Cox CM, Waud WR, Hartley JA, et al. SJG-136 (NSC 694501), a novel rationally designed DNA minor groove interstrand cross-linking agent with

potent and broad spectrum antitumor activity: part 2: efficacy evaluations. Cancer Res 2004;64:6700-6.

8. Hartley JA, Hamaguchi A, Coffils M, Martin CRH, Suggitt M, Chen Z, et al. SG2285, a novel C2-Aryl-substituted pyrrolobenzodiazepine dimer prodrug that cross-links DNA and exerts highly potent antitumor activity. Cancer Res 2010;70:6849-58.
9. Janjigian YY, Lee W, Kris MG, A phase 1 trial of SJG-136(NSC694501) in advanced solid tumors. Cancer Chemother Pharmacol 2010;65:833-8.
10. Stein AS, Walter RB, Erba HP, Fathi AT, Advani AS, Lancet JE, et al. A phase 1 trial of SGN-CD33A as monotherapy in patients with CD33-positive acute myeloid leukemia (AML). Blood 2015;126(23):324-.
11. Rudin CM, Pietanza MC, Bauerv TM, Spigel DR, Ready N, et al. Safety and efficacy of single-agent rovalpituzumab tesirine (SC16LD6.5), a delta-like protein 3 (DLL3)-targeted antibody-drug conjugate (ADC) in recurrent or refractory small cell lung cancer (SCLC). J Clin Oncol 2016;34 (suppl;abstr LBA8505).
12. Powell SN, Kachnic LA. Roles of BRCA1 and BRCA2 in homologous recombination, DNA replication fidelity and the cellular response to ionizing radiation. Oncogene 2003;22:5784-91.
13. Kobayashi H, Ohno S, Sasaki Y, Matsuura M. Hereditary breast and ovarian cancer susceptibility genes (review). Oncol Rep 2013;30:1019-29.
14. Russo A, Calo V, Bruno L, Rizzo S, Bazan V, Di Fede G. Herditary ovarian cancer. Crit Rev Oncol Hematol 2009;69:28-44.
15. Hucl T, Rago C, Gallmeier E, Brody JR, Gorospe M, Kern SE. A syngeneic variance library for functional annotation for human variant: application to *BRCA2*. Cancer Res 2008;68:5023-30.

16. Evers B, Drost R, Schut E, de Bruin M, van der Burg E, Derksen PW, et al. Selective inhibition of BRCA2-deficient mammary tumor cell growth by AZD2281 and cisplatin. Clin Cancer Res 2008;14:3914-25.

17. Ame JC, Spenlehaur C, de Murcia G. The PARP superfamily. Bioessays 2004;26:882-893.

18. Bryant HE, Schultz N, Thomas HD, Parker KM, Flower D, Lopez E, et al. Specific killing of *BRCA2*-deficienct tumors with inhibitors of poly(ADP-ribose) polymerase. Nature 2005;434:913-7.

19. Farmer H, McCabe N, Lord CJ, Tutt AJ, Johnson DA, Richardson TB, et al. Targeting the DNA repair defect in *BRCA* mutant cells as a therapeutic strategy. Nature 2005;434:917-21.

20. Gelmon KA, Tischkowitz M, Mackay H, Swenerton K, Robidoux A, Tonkin K, et al. Olaparib in patients with recurrent high-grade serous or poorly differentiated ovarian carcinoma or triple-negative breast cancer: a phase 2, multicentre, open-label, non-randomised study. Lancet Oncol 2011;12:852-61.

21. Marulonis UA, Harter P, Gourley C, Friedlander M, Vergote I, Rustin G, et al. Olaparib maintenance therapy in patients with platinum-sensitive, relapsed serous ovarian cancer and a BRCA mutation: overall survival adjusted for postprogression poly(adenosine diphosphate ribose) polymerase inhibitor therapy. Cancer 2016;122:1844-52.

22. Kristeleit R, Shapiro GI, Burris HA, Oza AM, LoRusso PM, et al. A phase I-II study of the oral poly(ADP-ribose) polymerase inhibitor rucaparib in patients with germline BRCA1/2-mutated ovarian carcinoma or other solid tumors. Clin Cancer Res 2017. pii: clincanres.2796.2016. doi: 10.1158/1078-0432.CCR-16-2796.

23. Solmlo G, Frankel P, Arun B, Ma CX, Garcia A, et al. Efficacy of the PARP inhibitor veliparib with carboplatin or as a single agent in patients with germline BRCA1- or

BRCA2-associated metastatic breast cancer. Clin Cancer Res 2017. pii: clincanres.2714.2016. doi: 10.1158/1078-0432.CCR-16-2714.

24. de Bono J, Ramanathan RK, Mina L, Chugh R, Glaspy J, et al. Phase I, dose-escalation, two-part trial of the PARP inhibitor talazoparib in patients with advanced germline BRCA1/2 mutations and selected sporadic cancers. Cancer Discov 2017 Feb 27. doi: 10.1158/2159-8290.CD-16-1250.

25. Scott LJ. Niraparib: First Global Approval. Drugs 2017 May 4. doi: 10.1007/s40265-017-0752-y. [Epub ahead of print]

26. Ledermann J, Harter P, Gourley C, Friedlander M, Vergote I, Rustin G, et al. Olaparib maintenance therapy in platinum-sensitive relapsed ovarian cancer. N Engl J Med 2012;366:1382-92.

27. Ledermann J, Harter P, Gourley C, Friedlander M, Vergote I, Rustin G, et al. Olaparib maintenance therapy in patients with platinum-sensitive relapsed serous ovarian cancer: a preplanned retrospective analysis of outcomes by BRCA status in a randomised pahse 2 trial. Lancet Oncol 2014;15:852-61.

28. Kummar S, Fleming GF, Oza AM, Sullivan DM, Gandara DR, Naughton M, et al. Randomized trial of oral cyclophosphamide and veliparib in high-grade serous ovarian cancer. Clin Cancer Res 2015;21:1574-82.

29. Albert JM, Cao C, Kim KW, Willey CD, Geng L, Xiao D, et al. Inhibition of poly(ADP-ribose) polymerase enhances cell death and improves tumor growth delay in irradiated lung cancer models. Clin Cancer Res 2007;13:3033-3042.

30. Chatterjee P, Choudhary GS, Sharma A, Singh K, heston WD, Ciezki J, et al. PARP inhibition sensitizes to low dose-rate radiation TMPRSS2-ERG fusion gene-expressing and

PTEN-deficient prostate cancer cells. PloS One 2013;8(4):e60408. doi: 10.1371/journal.pone.0060408.

31. Barreto-Andrade JC, Efimova E, Mauceri HJ, Beckett MA, Sutton HG, Darga TE, et al. Response of human prostate cancer cells and tumors to combining PARP inhibition with ionizing radiation. Mol Cancer Ther 2011;10:1185-93.

32. Gani C, Coacklet C, Kumareswaran R, Schutze C, Krause M, Zafarana G, et al. In vivo studies of the PARP inhibitor, AZD-2281, in combination with fractionated radiotherapy: An exploration of the therapeutic ratio. Radiother Oncol 2015;116:486-494.

33. Rottenberga S, Jaspersa JE, Kersbergena A, van der Burg E, Nygren AO, Zander SA, et al. High sensitivity of BRCA1-deficient mammary tumors to the PARP inhibitor AZD2281 alone and in combination with platinum drugs. PNAS 2008;105:17079-84.

34. Cardillo TM, Sharkey RM, Rossi DL, Arrojo R, Mostafa AA, Goldenberg DM. Synthetic lethality exploitation by an anti-Trop-2-SN-38 antibody-drug conjugate, IMMU-132, plus PARP-inhibitors in BRCA1/2-wild-type triple-negative breast cancer. Clin Cancer Res 2017; 23(13):3405-3415.

35. Langmead B, Salzberg SL. Fast gapped-read alignment with Bowtie 2. Nat Methods 2012;9(4):357-9.

36. Harper J, Lloyd C, Dimasi N, Toader D, Marwood R, et al. Preclinical evaluation of MEDI0641, a pyrrolobenzodiazepine-conjugated antibody-drug conjugate targeting 5T4. Mol Cancer Ther 2017 May 18. doi: 10.1158/1535-7163.MCT-16-0825.

37. Konish H, Mohseni M, Tamaki A, Garay JP, Croessmann S, et al. Mutation of a single allele of the cancer susceptibility gene BRCA1 leads to genomic instability in human breast epithelial cells. PNAS 2011;108(43):17773-8.

38. Mah LJ, El-Osta Am Jaraguabbus TC. gammaH2AX: a sensitive molecular marker of DNA damage and repair. Leukemia 2010;24:679-86.

39. Byrski T, Dent R, Blecharz P, Foszczynska-Kloda M, Gronwald J, Huzarski T, et al. Results of a phase II open-label, non-randomized trial of cisplatin chemotherapy in patients with BRCA1-positive metastatic breast cancer. Breast Cancer Res 2012;14:R110.

40. Sutherland MS, Walter RB, Jeffrey SC, Burke PJ, Yu C, et al. SGN-CD33A: a novel CD33-targeting antibody-drug conjugate using a pyrrolobenzodiazepine dimer is active in models of drug-resistant AML. *Blood* 2013;122: 1455-63.

41. Hinrichs MJ, Ryan PM, Zheng B, Afif-Rider S, Yu X, Gunsior M, et al. Fractionated dosing improves preclinical therapeutic index of pyrrolobenzodiazepine-containing antibody drug conjugates. Clin Cancer Res 2017 23(19):5858-5868.45.

42. McCabe N, Turner NC, Lord CJ, Kluzek K, Bialkowska A, Swift S, et al. Deficiency in the repair of DNA damage by homologous recombination and sensitivity to poly(ADP-ribose) polymerase inhibition. Cancer Res 2006;66:8109-15.

43. Ip LRH, Poulogiannis G, Viciano FC, Sasaki J, Kofuji S, Spanswick VJ, et al. Loss of INPP4B causes a DNA repair defect through loss of BRCA1, ATM and ATR and can be targeted with PARP inhibitor treatment. Oncotarget 2015;6:10548-62.

Figure Legends

Figure 1. *In vivo* efficacy of 5T4-PBD in *BRCA* wild-type or *BRCA*-deficient cancer xenograft models. A single dose of 5T4-PBD was administrated at 0.1 and 0.3 mg/kg intravenously into nude mice bearing (A) BRCA wild-type tumors (MDA-MB-361, MDA-MB-468, NCI-H1975), or (B) BRCA-deficient tumors (Figure 1B: SUM149PT, MDA-MB-436, and Capan-1). 5T4 expression in tumor cell lines was determined by FACS analysis and annotated as 5T4 high, medium, and low.

Figure 2. Genetic deletion of *BRCA2* augments antitumor activity of PBD-based ADC *in vitro* and *in vivo*. A, Flow cytometric analysis of 5T4 surface expression in DLD1 parental and *BRCA2*-/- cells. B, dose-response curves from in *vitro* cell viability assays in DLD1 isogenic cells. Cell viability was calculated by normalizing to untreated cells. C, tumor volumes of DLD1 parental tumors (top panel) or DLD1 BRCA2-/- tumors (bottom panel) in nude mice administrated with single dose of 5T4-PBD intravenously at dose levels of 0.1, 0.3, 1 mg/kg. D, treatment with 5T4-PBD induces enhanced DNA damage in *BRCA2*-/- cells. Immunohistochemical staining of γH2AX (red) and DAPI (blue) in DLD1 wild-type or DLD1 BRCA2-/- cells treated with ADC dilution buffer or 5T4-PBD (10 or 100 ng/ml) for 24 hours. Graph represents quantitation of γH2AX formation using a γ-H2AX Pharmacodynamic Assay. P values were calculated by student T-test. E, western blot of HRR proteins expression in DLD1 and DLD1 *BRCA2*-/- cells.

Figure 3. Pharmacologic response to PBD-based ADC across *BRCA*-deficient PDX populations. 18 breast and 5 ovarian PDX models with *BRCA* mutations or deletions (n=2-3 mice per group) were treated intravenously with 5T4-PBD at (A) 0.3 mg/kg single dose, or (B)

0.1 mg/kg Q3W x 3 dosing regimen. Waterfall plots illustrate the best response indicated by percentage tumor volume change from baseline in all PDX tumors on study. Each untreated tumor was stained and scored for 5T4 expression. Colored bars represent individual tumors and colors correspond to the IHC scores. Solid bars are breast PDX models, and patterned bars are ovarian PDX models. IS: intensity score; FS: frequency score. Tumor growth curves on individual PDX models can be found in Supplemental Figure S3 & S4.

Figure 4. Effect of 5T4-PBD in combination with olaparib. A, *In vitro* cell viability assay of olaparib in DLD1 and DLD1 *BRCA2*-/- isogenic cells. B, *In vitro* cell viability assay testing the combination of 5T4-PBD with olaparib in DLD1 and DLD1 *BRCA2*-/- isogenic cells. Statistical significance was assessed using Student T-test. ***, p<0.001; *, p<0.05. C, combination of 5T4-PBD with olaparib in DLD1 xenograft model. 5T4-PBD (1 mg/kg) was given as single dose intravenously on day 9 post tumor implantation. olaparib (100 mg/kg) was dosed daily by oral gavage starting on day 9 ending on day 34. D, combination of 5T4-PBD with olaparib in DLD1 *BRCA2*-/- xenograft model. 5T4-PBD was dosed at 0.1 mg/kg on day 8. Olaparib was dosed daily by oral gavage staring on day 8 ending on day 35. Statistical significance was evaluated using two-way ANOVA. ****, p<0.0001.

Figure 5. Tolerability of 5T4-PBD in combination with olaparib in naïve nude mice. Single dose of 5T4-PBD (0.1 mg/kg) was administered on day 0. Olaparib (100 mg/kg) was given daily from day 0-15. Whole blood was collected via orbital bleeding on day 2, day 9, day 13, day 20, and day 27 for automated CBC determinations. Statistical significance was evaluated using Student T-test. *, p<0.05 versus untreated; **, p<0.01 versus untreated.

Figure 1.

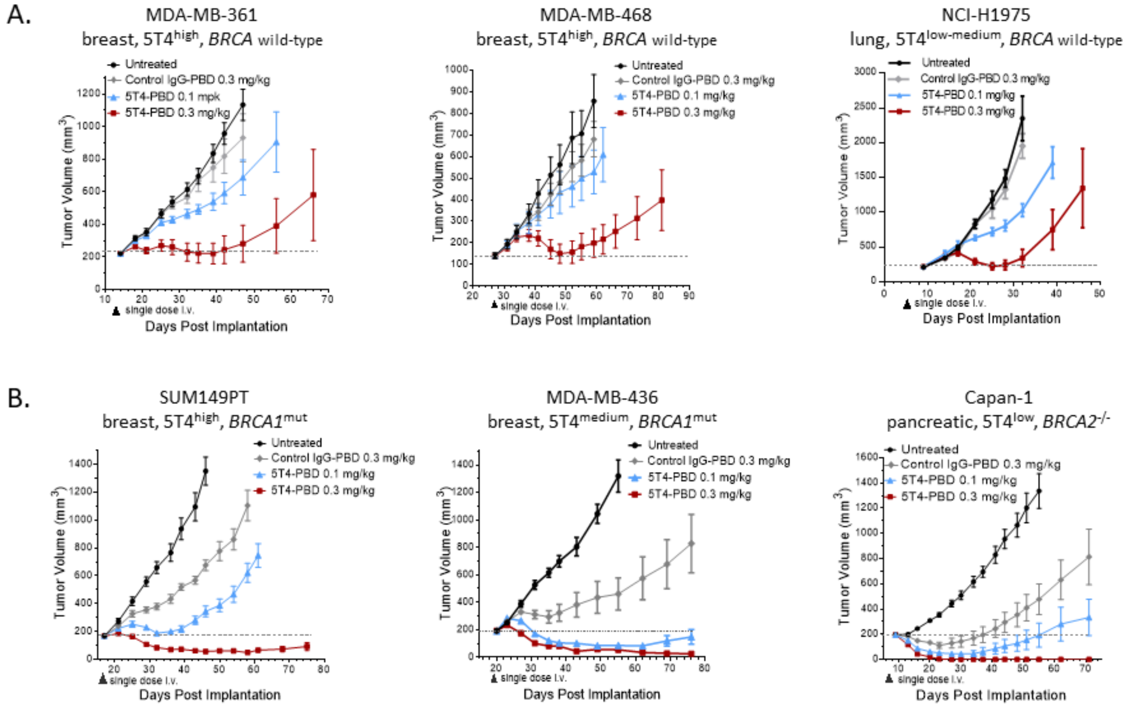
A.
MDA-MB-361
breast, 5T4high, BRCA wild-type
Untreated
Control IgG-PBD 0.3 mg/kg
5T4-PBD 0.1 mpk
5T4-PBD 0.3 mg/kg
Tumor Volume (mm3)
0
200
400
600
800
1000
1200
10
20
30
40
50
60
70
single dose i.v.
Days Post Implantation
MDA-MB-468
breast, 5T4high, BRCA wild-type
Untreated
Control IgG-PBD 0.3 mg/kg
5T4-PBD 0.1 mg/kg
5T4-PBD 0.3 mg/kg
Tumor Volume (mm3)
0
100
200
300
400
500
600
700
800
900
1000
20
30
40
50
60
70
80
90
single dose i.v.
Days Post Implantation
NCI-H1975
lung, 5T4low-medium, BRCA wild-type
Untreated
Control IgG-PBD 0.3 mg/kg
5T4-PBD 0.1 mg/kg
5T4-PBD 0.3 mg/kg
Tumor Volume (mm3)
0
500
1000
1500
2000
2500
3000
0
10
20
30
40
50
single dose i.v.
Days Post Implantation
B.
SUM149PT
breast, 5T4high, BRCA1mut
Untreated
Control IgG-PBD 0.3 mg/kg
5T4-PBD 0.1 mg/kg
5T4-PBD 0.3 mg/kg
Tumor Volume (mm3)
0
200
400
600
800
1000
1200
1400
20
30
40
50
60
70
80
single dose i.v.
Days Post Implantation
MDA-MB-436
breast, 5T4medium, BRCA1mut
Untreated
Control IgG-PBD 0.3 mg/kg
5T4-PBD 0.1 mg/kg
5T4-PBD 0.3 mg/kg
Tumor Volume (mm3)
0
200
400
600
800
1000
1200
1400
20
30
40
50
60
70
80
single dose i.v.
Days Post Implantation
Capan-1
pancreatic, 5T4low, BRCA2-/-
Untreated
Control IgG-PBD 0.3 mg/kg
5T4-PBD 0.1 mg/kg
5T4-PBD 0.3 mg/kg
Tumor Volume (mm3)
0
200
400
600
800
1000
1200
1400
1600
10
20
30
40
50
60
70
single dose i.v.
Days Post Implantation

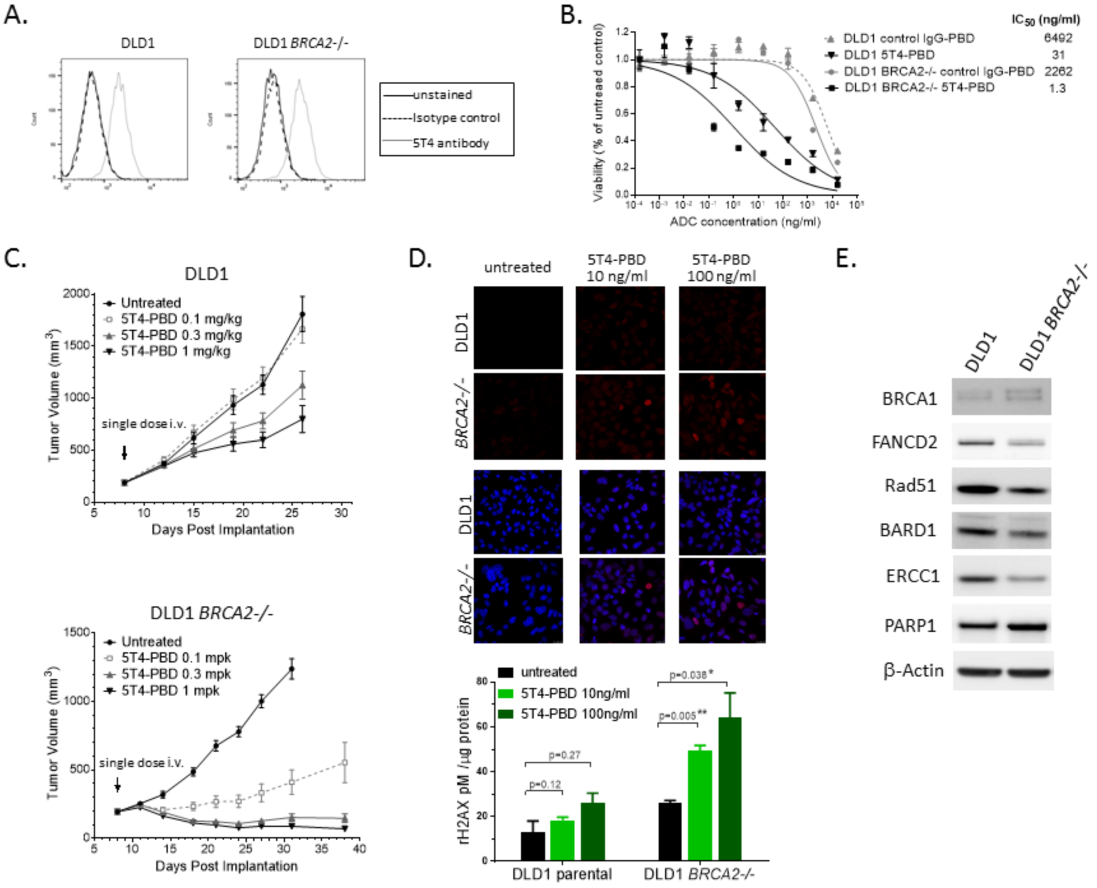
A.
DLD1
DLD1 *BRCA2-/-*
unstained
Isotype control
5T4 antibody
B.
IC50 (ng/ml)
DLD1 control IgG-PBD 6492
DLD1 5T4-PBD 31
DLD1 BRCA2-/- control IgG-PBD 2262
DLD1 BRCA2-/- 5T4-PBD 1.3
Viability (% of untreaed control)
ADC concentration (ng/ml)
C.
DLD1
Untreated
5T4-PBD 0.1 mg/kg
5T4-PBD 0.3 mg/kg
5T4-PBD 1 mg/kg
single dose i.v.
Tumor Volume (mm3)
Days Post Implantation
DLD1 *BRCA2-/-*
Untreated
5T4-PBD 0.1 mpk
5T4-PBD 0.3 mpk
5T4-PBD 1 mpk
single dose i.v.
Tumor Volume (mm3)
Days Post Implantation
D.
untreated
5T4-PBD 10 ng/ml
5T4-PBD 100 ng/ml
DLD1
BRCA2-/-
DLD1
BRCA2-/-
untreated
5T4-PBD 10ng/ml
5T4-PBD 100ng/ml
p=0.12
p=0.27
p=0.005**
p=0.038*
rH2AX pM /µg protein
DLD1 parental
DLD1 *BRCA2-/-*
E.
DLD1
DLD1 *BRCA2-/-*
BRCA1
FANCD2
Rad51
BARD1
ERCC1
PARP1
β-Actin

Figure 2.

Figure 3.

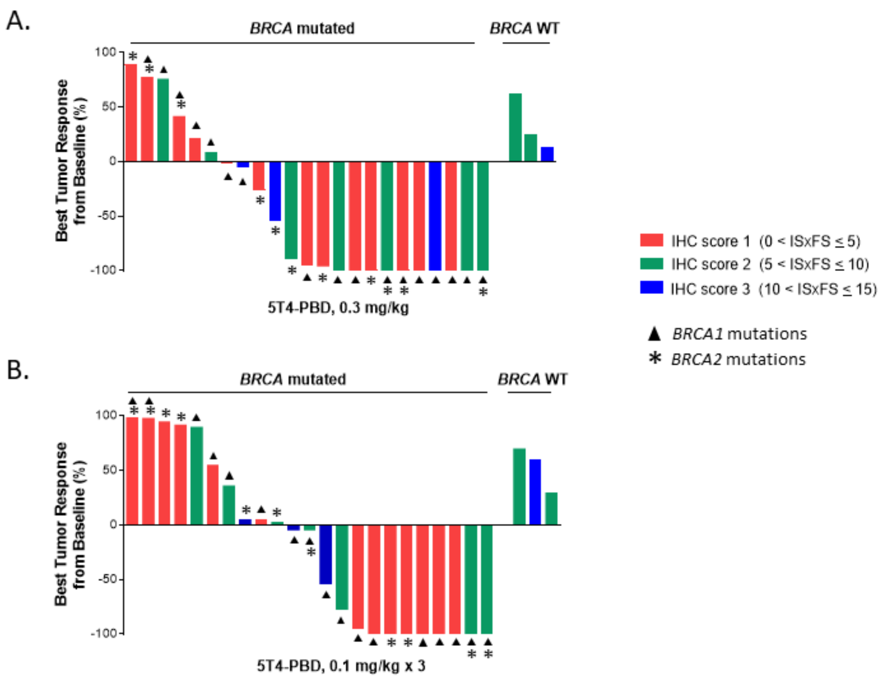
A.
BRCA mutated
BRCA WT
Best Tumor Response from Baseline (%)
100
50
0
-50
-100
5T4-PBD, 0.3 mg/kg
B.
BRCA mutated
BRCA WT
Best Tumor Response from Baseline (%)
100
50
0
-50
-100
5T4-PBD, 0.1 mg/kg x 3
🟥 IHC score 1 (0 < ISxFS ≤ 5)
🟩 IHC score 2 (5 < ISxFS ≤ 10)
🟦 IHC score 3 (10 < ISxFS ≤ 15)
▲ *BRCA1* mutations
∗ *BRCA2* mutations

Figure 4.

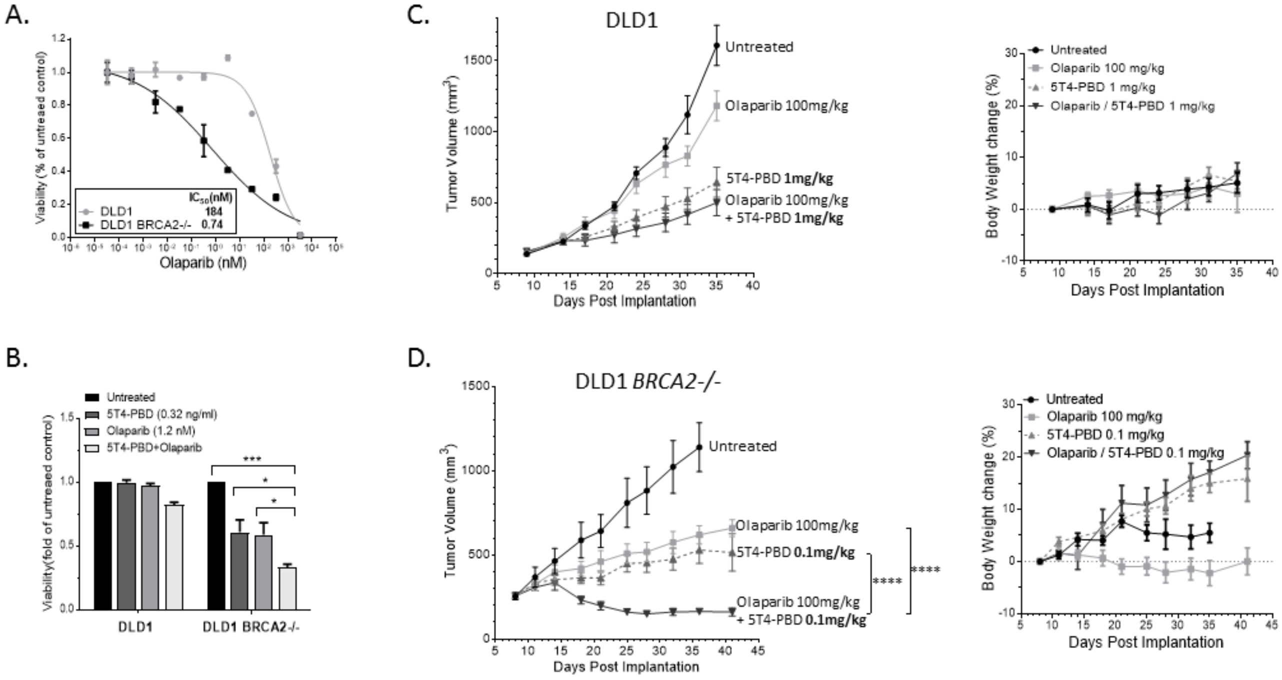
A.
Viability (% of untreaed control)
1.2
1.0
0.8
0.6
0.4
0.2
0.0
IC50(nM)
DLD1 184
DLD1 BRCA2-/- 0.74
10⁻⁶ 10⁻⁵ 10⁻⁴ 10⁻³ 10⁻² 10⁻¹ 10⁰ 10¹ 10² 10³ 10⁴ 10⁵
Olaparib (nM)
B.
Untreated
5T4-PBD (0.32 ng/ml)
Olaparib (1.2 nM)
5T4-PBD+Olaparib
Viability(fold of untreaed control)
1.5
1.0
0.5
0.0
***
*
*
DLD1
DLD1 BRCA2-/-
C.
DLD1
Tumor Volume (mm3)
1500
1000
500
0
Untreated
Olaparib 100mg/kg
5T4-PBD 1mg/kg
Olaparib 100mg/kg
+ 5T4-PBD 1mg/kg
5 10 15 20 25 30 35 40
Days Post Implantation
Body Weight change (%)
30
20
10
0
-10
Untreated
Olaparib 100 mg/kg
5T4-PBD 1 mg/kg
Olaparib / 5T4-PBD 1 mg/kg
5 10 15 20 25 30 35 40
Days Post Implantation
D.
DLD1 BRCA2-/-
Tumor Volume (mm3)
1500
1000
500
0
Untreated
Olaparib 100mg/kg
5T4-PBD 0.1mg/kg
Olaparib 100mg/kg
+ 5T4-PBD 0.1mg/kg
****
****
5 10 15 20 25 30 35 40 45
Days Post Implantation
Body Weight change (%)
30
20
10
0
-10
Untreated
Olaparib 100 mg/kg
5T4-PBD 0.1 mg/kg
Olaparib / 5T4-PBD 0.1 mg/kg
5 10 15 20 25 30 35 40 45
Days Post Implantation

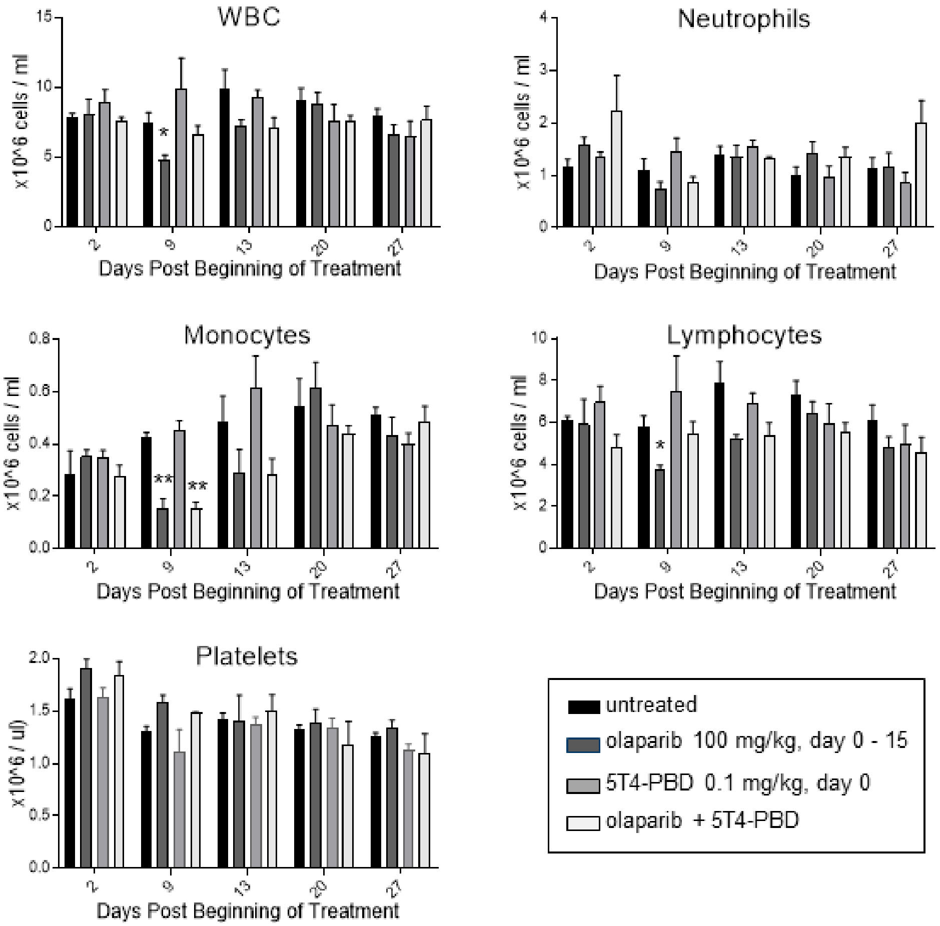
WBC
x10^6 cells / ml
0
5
10
15
2
9
13
20
27
Days Post Beginning of Treatment
*
Neutrophils
x10^6 cells / ml
0
1
2
3
4
2
9
13
20
27
Days Post Beginning of Treatment
Monocytes
x10^6 cells / ml
0.0
0.2
0.4
0.6
0.8
2
9
13
20
27
**
**
Days Post Beginning of Treatment
Lymphocytes
x10^6 cells / ml
0
2
4
6
8
10
*
2
9
13
20
27
Days Post Beginning of Treatment
Platelets
x10^6 / ul)
0.0
0.5
1.0
1.5
2.0
2
9
13
20
27
Days Post Beginning of Treatment
untreated
olaparib 100 mg/kg, day 0 - 15
5T4-PBD 0.1 mg/kg, day 0
olaparib + 5T4-PBD

Figure 5.

AACR American Association for Cancer Research

Molecular Cancer Therapeutics

Improved therapeutic window in BRCA mutant tumors with antibody linked pyrrolobenzodiazepine dimers with and without PARP inhibition

Haihong Zhong, Cui Chen, Ravinder Tammali, et al.

Mol Cancer Ther Published OnlineFirst October 23, 2018.